Proceedings of the XVII ECSMGE-2019
Geotechnical Engineering foundation of the future
ISBN 978-9935-9436-1-3

doi: 10.32075/17ECSMGE-2019-0909

XVII European Conference
ECSMGE 2019
Reykjavik
on Soil Mechanics
and Geotechnical Engineering

The application of limit analysis to the study of the basal failure of deep excavations in clay considering the spatial distribution of soil strength

Application de l'analyse limite à l'étude de la rupture de la base d'excavations en argiles considérant la distribution spatiale de la résistance du sol

L. A. Viana
NOVA University of Lisbon, Lisbon, Portugal

A. N. Antão, M. Vicente da Silva, N. M. C. Guerra
UNIC, NOVA University of Lisbon, Lisbon, Portugal

ABSTRACT: Deterministic calculations are a traditional way of determining the limit loads of geotechnical problems. Over the last two decades, probabilistic methods have increasingly been applied to such problems. In this paper, the finite element program *mechpy*, developed by the authors' team, is adapted to, firstly, generate samples of the spatial pattern of the undrained shear strength using the log-normal distribution and, secondly, perform upper- and lower-bound limit analysis calculations using those samples. This procedure is applied to determine the mean basal stability number in several cases with different geometries and representative values of the undrained shear strength standard deviation and of the scale of fluctuation. The basal stability numbers obtained are compared with those from the corresponding deterministic calculations.

RÉSUMÉ: Les calculs déterministes sont un moyen traditionnel de déterminer les charges limites des problèmes géotechniques. Au cours des deux dernières décennies, les méthodes probabilistes ont été de plus en plus appliquées à ces problèmes. Dans cet article, le logiciel d'éléments finis *mechpy*, développé par l'équipe de recherche des auteurs, est adapté pour, premièrement, générer des échantillons de la distribution spatiale de la résistance au cisaillement non drainée en utilisant la distribution log-normale et, deuxièmement, effectuer des calculs d'analyse limite (limites supérieure et inférieure) en utilisant ces échantillons. Cette procédure est appliquée à déterminer la moyenne du nombre de stabilité basale dans quelques cas avec des géométries différentes et des valeurs représentatives de la variabilité type de la résistance au cisaillement non drainée et de l'échelle de fluctuation. Les nombres de stabilité basale obtenus sont comparés à ceux des calculs déterministes correspondants.

Keywords: limit analysis; basal failure; soil spatial variability; probabilistic analysis

1 INTRODUCTION

The basal failure of deep excavations is a stability problem involving the collapse of a large mass of soil. In the present work, the loads leading to collapse will be determined through *mechpy*, a program for automatic calculation of collapse load approximations using limit analysis and the finite element method. The basal failure of deep excavations in clay is, in this work, analysed in total stresses, and the undrained shear strength

(c_u) is thus considered. The stochastic behaviour of soil properties can be of great relevance on the engineering problem under consideration, since different distributions of the soil strength might lead to completely different failure mechanisms and, therefore, different values of the collapse load (which will, in turn, lead to different values of the basal stability number). For this reason, the program *mechpy* was adapted to, firstly, generate samples of the spatial pattern of the undrained shear strength using the log-normal distribution and, then, considering an associated plastic flow rule and a rigid-plastic behaviour, perform upper- and lower-bound limit analysis calculations using those samples. A previous version of *mechpy* has already been used by Simões et al. (2012) to determine upper-bounds for the 2D and 3D bearing capacity problem on random fields. The soil variability is modelled by random fields, varying its undrained shear strength according to the coefficient of variation and the correlation length (scale of fluctuation). Said random fields are simulated using the Latin Hypercube Sampling (LHS) method.

The probabilistic analysis of geotechnical engineering projects requires the probabilistic characterization of the soil and, consequently, the study of geotechnical uncertainties, as well as the sources of geotechnical variability. Uncertainty in geotechnical engineering can be categorized into aleatoric, epistemic and decision model uncertainties (Van Gelder, 2000; Hartford and Baecher, 2004; Huber, 2013). This study takes the spatial distribution of soil strength, i.e., the natural variability of c_u from point to point within a soil volume, into consideration. Said natural variability or physical uncertainty (aka inherent uncertainty or intrinsic uncertainty) is an aleatoric uncertainty, which cannot be reduced on increasing site investigation (Veritas, 2012).

2 PROBLEM

The problem under consideration in the present work is the basal stability of a deep excavation in clay. The excavation is performed in an isotropic single-layer soil under undrained conditions and is analysed in 2D plane strain conditions. Its geometric characteristics are shown in Figure 1, where h is the excavation height, B is the excavation width, d is the distance between the bottom of the excavation and the rigid stratum and ls, A and C will be described further in the paper.

It should be noted that although 2D problems in plane strain state are common in geotechnical analyses, for the problem under consideration this simplification is a limitation of the present work since it results in a homogenisation of the soil properties in the perpendicular axis.

The basal stability of deep excavations in clay in 2D problems is analysed using a basal stability number N_s, a dimensionless coefficient depending on h/B and d/h ratios :

$$N_s = \frac{\gamma h}{c_u} \qquad (1)$$

with γ being the average total unit weight.

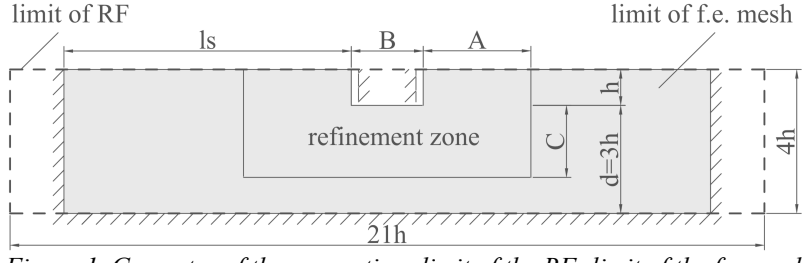

Figure 1. Geometry of the excavation; limit of the RF; limit of the f.e. mesh

3 SPATIAL VARIABILITY OF c_u

According to Vanmarcke (1977), the spatial variability can be modelled as a random field (RF), which requires some parameters to characterize it: the standard deviation (σ), the mean (μ) and the auto-correlation function (ACF). A dimensionless representation of inherent soil variability can be obtained by normalising the standard deviation with respect to the mean value of the soil property, leading to the coefficient of variation of inherent soil variability (cov). Based on the literature (Lee et al., 1983; Phoon and Kulhawy, 1999), a range of values for the coefficient of variation of the undrained shear strength was established: $cov_{c_u} \in [0.1,1]$.

Another statistical parameter needed to describe the inherent soil variability is the correlation length (θ), aka the scale of fluctuation. As described by Fenton and Griffiths (2008), θ is the distance within which points are significantly correlated (i.e. by more than about 10%). In other words, it describes the maximum distance to which the spatial distribution of the random variable is expected to be correlated and a high value of such parameter implies a highly correlated distribution of the undrained shear strength in the elements of the RF mesh. Based on the literature (Phoon and Kulhawy, 1999), a range of values for the correlation length of c_u in the horizontal and vertical directions was established: $\theta_{H,c_u} \in [46m, 60m]$; $\theta_{V,c_u} \in [2m, 6.2m]$. However, an isotropic spatial correlation structure ($\theta_V = \theta_H$, i.e. a statistically isotropic RF) was considered in the present work for the sake of simplification.

4 GENERATION OF RANDOM FIELDS

As previously stated, in the present work the generation of the random fields is based on the LHS method, which is a numerical simulation method for generating a near-random sample of parameter values from a multidimensional distribution. It is widely used in Monte Carlo simulation because it can greatly reduce variance, leading to the same level of accuracy with fewer samples (simulations, program runs). The underlying concept of this method is based on the principle of dividing the sample space of each variable into equiprobable intervals, each of which is sampled only once. The numerical implementation of the LHS method used follows Olsson et al. (2003).

The sampled field has dimensions $21h \times 4h$ and is schematically represented in Figure 1 by the limit of RF. Each spatial distribution of c_u is modelled using a uniform RF mesh comprised of equal sized square elements, to which different values of c_u are assigned using the LHS method. The RF mesh coarseness is defined by the parameter sm_{RF}; some examples are presented in the following section in Figure 3.

The spatial correlation of soil properties is determined based on the ACF adopted, which is given by:

$$\boldsymbol{\rho_{ln\,c_u}(\tau) = exp\left(-\frac{2|\tau|}{\theta_{ln\,c_u}}\right)} \qquad \textit{(2)}$$

where $\rho_{ln\,c_u}$ is the correlation coefficient between the properties of two elements of the RF mesh, τ is the distance between the centre of mass of these elements and $\theta_{ln\,c_u}$ is the correlation length of the undrained shear strength of the soil, which will be generically referred as θ_{c_u} from now on. Note that ρ falls exponentially with increasing distance.

Based on the LHS method, samples with normal distribution, zero mean, unit standard deviation and a spatial correlation length θ_{c_u} are generated. From this normal distribution c_u^*, a log-normal distribution is obtained for c_u by the following expression:

$$\boldsymbol{c_{u_{ij}} = exp\,(\mu_{ln\,c_u} + \sigma_{ln\,c_u} c^*_{u_{ij}})} \qquad \textit{(3)}$$

where $c_{u_{ij}}$ is the c_u value assigned to the element j in sample i, $\mu_{ln\,c_u}$ and $\sigma_{ln\,c_u}$ correspond to the mean and standard deviation of the log-normal

distribution for c_u, which are obtained by the following equations, respectively:

$$\sigma_{ln\,c_u} = \sqrt{ln\left(1 + \frac{\sigma_{c_u}^2}{\mu_{c_u}^2}\right)} \quad (4)$$

$$\mu_{ln\,c_u} = ln\,(\mu_{c_u}) - 0.5\,\sigma_{ln\,c_u}^2 \quad (5)$$

The previously mentioned samples are used to model the RF that simulates the distribution of c_u. Moreover, the probabilistic characterization of c_u is fully defined by equation 3, which is dependent on three parameters: $\mu_{ln\,c_u}$, $\sigma_{ln\,c_u}$ and θ_{c_u}. As previously stated, the coefficient of variation, a dimensionless parameter, is used:

$$cov_{c_u} = \frac{\sigma_{c_u}}{\mu_{c_u}} \quad (6)$$

In order to study the influence of some probabilistic and geometric properties on the basal failure of deep excavations in clay, a parametric analysis is performed. For this purpose, sets of samples are generated using the following values:
$\mu_{c_u} = 200kPa$; $cov_{c_u} = [0.1, 0.25, 0.5, 1]$; $\theta_{c_u} = [2m, 10m, 20m, 40m, 80m]$; $sm_{RF} = 0.2h$.

For the given μ_{c_u} and a given pair of values of cov_{c_u} and θ_{c_u} a set of samples is generated using the RF mesh. As a result of the application of the LHS method, the number of samples has to be higher than the number of random variables, which in this case is equal to the number of elements of the RF mesh: 2100 (105x20); the number of samples is taken equal to 2101.

5 NUMERICAL ANALYSIS

Each one of the samples generated for the given μ_{c_u} and a given pair of values of cov_{c_u} and θ_{c_u} using the RF mesh undergoes a process of mapping with a finite element (f.e.) mesh corresponding to a given geometry. It should be noted that each set of samples corresponding to the given μ_{c_u} and a given pair of cov_{c_u} and θ_{c_u} is generated only once, but is used with different f.e. meshes; simulating a soil (analysed by means of probabilistic methods) that would be subjected to different excavations geometries.

The schematic representation of the f.e. mesh is shown in Figure 1 and is defined by h, B, d and ls. The f.e. mesh domain is less than or equal to the limit of the RF (Table 1).

The f.e. mesh is comprised of regular triangular elements and its coarseness is defined by the parameter sm_{fe}, equal to $0.2h$. A refined area around the excavation was considered as is defined by A and C (Figure 1; Table 1). The refinement factor of 2 was applied to this zone.

Table 1. Geometric values adopted for the f.e. mesh in the parametric analysis

$h(m)$	d/h	h/B	ls/h	A/h	C/h
10	3	0.2	8	0	0
10	3	0.5	8	3	2
10	3	1	6	3	2
10	3	2	5	2	1.5

In order to improve computing time, ls, A and C values were adapted to each h/B ratio. The $d/h = 3$ ratio was chosen because it corresponds to a deep rigid stratum in the homogeneous case for all h/B ratios except for 0.2. Considering a deeper rigid stratum would result in larger f.e. meshes and, consequently, a larger RF mesh, which would lead to greater computing time.

The boundary conditions adopted for the f.e. mesh consist of preventing vertical and horizontal displacements at the base and at the left and right edges of the domain, as shown in Figure 1. The horizontal displacement of the vertical faces of the excavation was also prevented in order to simulate the effect of the retaining wall, which was not modelled.

The f.e. meshes resulting from the mapping process are used to perform upper- and lower-bound limit analysis calculations. These sets of deterministic calculations are used to determine

the mean basal stability number for each case of the parametric analysis and separately for upper- and lower-bound:

$$\mu_{N_s} = \frac{1}{2101}\sum_{i=1}^{2101}\frac{\gamma_{c;i}\,h}{\mu_{c_u}} \qquad (7)$$

where $\gamma_{c;i}$ is the unit weight leading to the collapse of the i-th sample.

It should be noted that sensitivity analyses have shown that the f.e. mesh refinement has a great impact on the results of $\gamma_{c;i}$ and, consequently, on the mean basal stability number; which in turn affects the gap between the upper- and lower-bound solutions.

The homogeneous case was also numerically analysed using the same f.e. tool. The f.e. meshes are the same as the ones for the calculations with the random soil properties. Figure 2 compares the values obtained for the homogeneous case with those presented by Santana et al. (2018), also obtained using *mechpy* and defined by the maximum of the following equations, which were obtained for $h/B \in [0.2, 3]$ and $d/h \in [1/3, 3]$:

$$\frac{\gamma h}{c_u} = (2+\pi)\left\{1 + 0.815\,arctan\left[0.359\left(\frac{h}{B}\right)^{0.55}\right]\right\} \qquad (8)$$

$$\frac{\gamma h}{c_u} = 1 + \pi + exp\left[-0.409 + 1.275\left(\frac{d}{h}\right)^{-0.246}\right] \qquad (9)$$

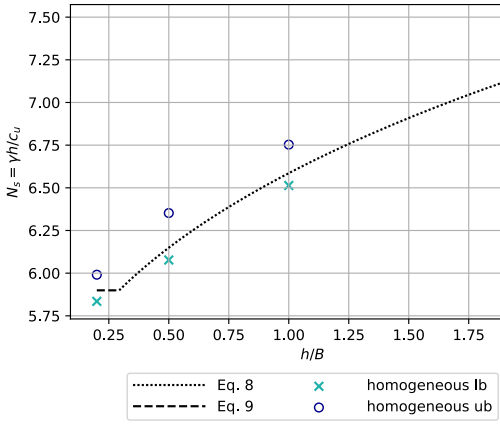

Figure 2. Basal stability number for the homogeneous case; Eq. 9 for d/h=3

Results show some differences between the UB and LB values, which is due to the fact that the meshes used can not be as refined as the ones that lead to the solution included in Figure 2. The reason for this is the large computing time such refined meshes would take, as the study presented in this paper involved 336000 calculations for the random field analysis.

6 RESULTS

Figure 3 shows some examples of RF and plastic deformation zones for $h/B = 0.5$ obtained for two values of cov_{c_u} and two values of θ_{c_u}.

From an overall analysis of Figure 3, one can see that the soil variability shows a great influence on the failure mechanisms, be it in dimension or in geometry. Failure mechanisms of cases corresponding to soils characterised by high cov_{c_u} values are less likely to be close to the ones from a homogeneous soil.

It is also interesting to note that whereas $d/h = 3$ corresponds to a deep rigid stratum in the homogeneous case (which does not affect the mechanism), the same is not always true in the RF approach.

As previously mentioned, it was found that the f.e. mesh coarseness plays an important role on the failure mechanism. Therefore, the f.e. mesh was refined in a zone adjacent to the excavation, and as this refinement increases, the patterns of the plastic deformation zone obtained from the UB and LB calculations become increasingly similar to one another; in turn, makes the gap between their μ_{N_s} values much tighter.

Figure 4 shows the results obtained for the mean basal stability number for several cases with different geometries and cov_{c_u} and θ_{c_u}. The lower the h/B ratio, the tighter the gap between the UB and LB solutions for μ_{N_s}. It should be noted that the results presented for $h/B = 0.2$ seem to contradict this behaviour, but it is only due to the fact that in this particular case the

refinement zone of the f.e. mesh does not exist and so the mesh is coarser than in the other cases, which indeed leads to slightly worse results.

It can also be seen that, the lower the cov_{c_u}, the greater the μ_{N_s} values and the lower their oscillation, drawing increasingly near the results

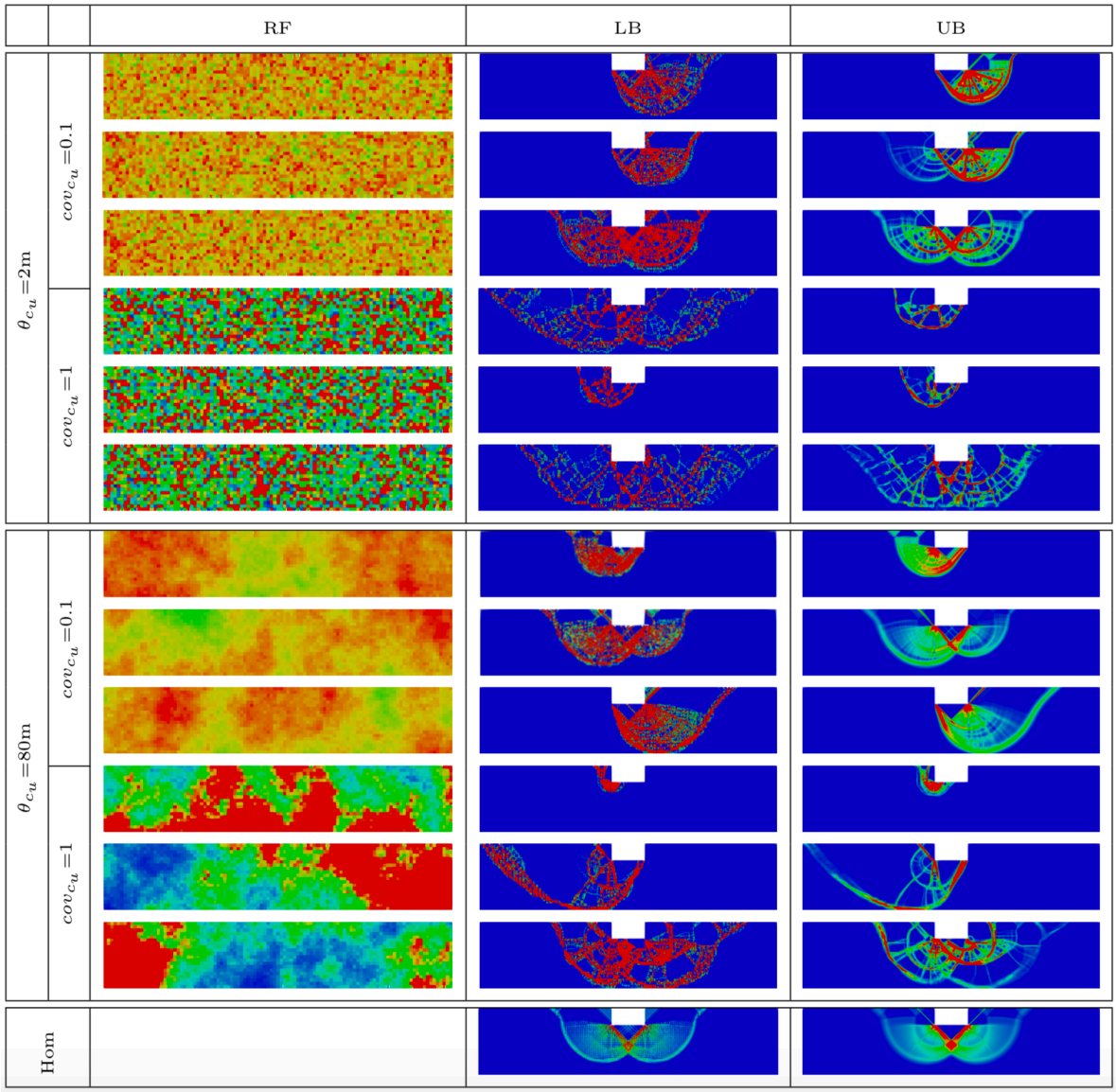

Figure 3. Some examples of Random fields (RF) and plastic deformation zones obtained for different pairs of cov_{c_u} *and* θ_{c_u} *values for* $h/B = 0.5$*; plastic deformation zones obtained for the homogeneous case for* $h/B = 0.5$*. It should be noted that the red squares in RF represent* c_u *values equal or greater than 500kPa.*

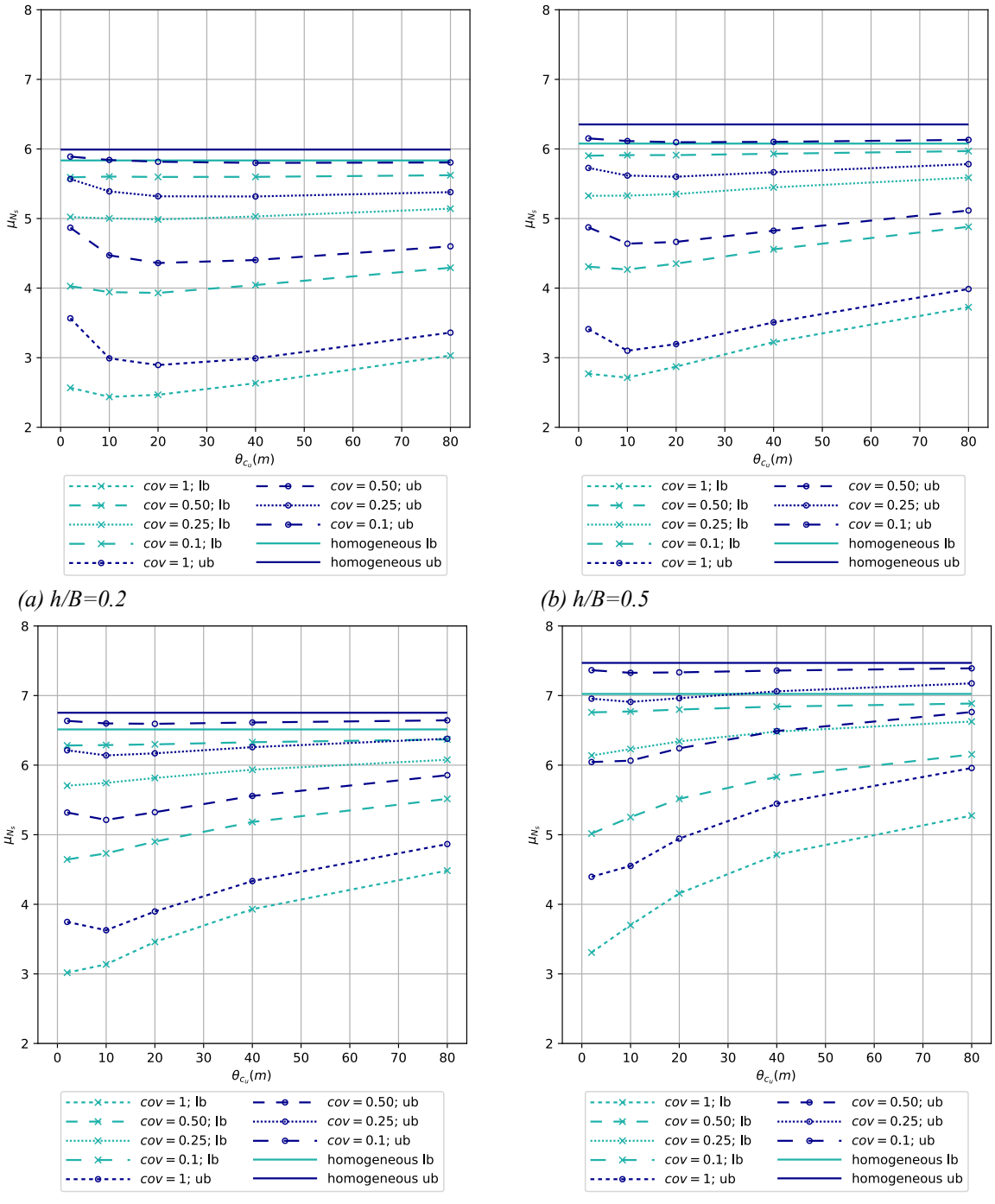

(a) h/B=0.2 *(b) h/B=0.5*

(c) h/B=1.0 *(d) h/B=2.0*

Figure 4. Mean basal stability number for different geometries for the homogeneous case and for different coefficient of variation and scale of fluctuation values

of the homogeneous case. Such results would be expected since lower coefficients of variation represent less heterogeneous soils.

In Figure 4(a), one can see that as θ_{c_u} decreases, the μ_{N_s} curve goes down, but only up to a certain point, where it rises again; showing an upward curvature. This result goes in line with Fenton and Griffiths (2008) findings. It can also be noted that said curvature is more evident in the UB solutions and the lower the h/B ratio. Indeed, not only do Figures 4(c) and (d) present cases where the evolution of μ_{N_s}values does not show an inversion (even for high cov_{c_u}values), but they also present cases in which μ_{N_s} values show steady growth with the increase of θ_{c_u}, now showing a downward curvature. However, such observations may be due to the fact that the results obtained for low h/B ratios are comparatively worse, which can be explained by the fact that low h/B ratios may require an even greater f.e. mesh refinement. Forthcoming works will dwell on this problem.

The parameter θ_{c_u} has more effect on narrow excavations, which is more evident for high cov_{c_u} values. Such result would be expected and is due to the scale between θ_{c_u} and the excavation geometry.

7 CONCLUSIONS

The mean basal stability numbers obtained when considering the variability of soil properties are smaller than the ones for the homogeneous cases. This fact is also observed for other stability problems such as bearing capacity of foundations.

Variability of soil properties results in a wide variety of failure mechanisms. For the cases analysed, cov_{c_u} has a greater influence on the stability number when in comparison with the scale of fluctuation. The influence of the scale of fluctuation is greater for greater cov_{c_u}. For larger values of θ_{c_u}, variability has a greater influence on smaller h/B ratios.

8 REFERENCES

Fenton, G.A., Griffiths, D.V. 2008. *Risk assessment in geotechnical engineering*, John Wiley & Sons.

Hartford D.N.D., Baecher, G.B. 2004. *Risk and Uncertainty in Dam Safety*, Thomas Telford Ltd, London.

Huber, M. 2013. *Soil Variability and its Consequences in Geotechnical Engineering*, Universitat Stuttgart, Germany.

Lee, I.K., White, W., Ingles, O.G. 1983. *Geotechnical Engineering*, Pitman, London.

Olsson, A., Sandberg, G., Dahlblom, O. 2003. On Latin hypercube sampling for structural reliability analysis, *Structural Safety* **25**, 47–68.

Phoon, K.-K., Kulhawy, F.H. 1999. Characterization of geotechnical variability, *Canadian Geotechnical Journal* **36**, 612–624.

Santana, T., Vicente da Silva, M., Antão, A.N., Guerra, N.M.C. 2018. Two-dimensional upper- and lower-bound numerical analysis of the basal stability of deep excavations in clay. *Numerical Methods in Geotechnical Enginnering IX*, Porto, Cardoso et al. (Eds), 1197-1202, Taylor and Francis, London.

Simões, J.T., Neves, L.C., Antão, A.N., Guerra, N.M.C. 2012. Two-dimensional probabilistic study of bearing capacity of shallow foundations on undrained soil. *Pensar e Construir com a Natureza. Uma Visão para a Engenharia: Proceedings, 13th CNG.* Lisbon. In Portuguese.

Van Gelder, P.H.A.J.M. 2000. *Statistical methods for the risk-based design of civil structures*, Delft University of Technology, Netherlands.

Vanmarcke, E.H. 1977. Probabilistic modeling of soil profiles, *Journal of Geotechnical Engineering Division, ASCE,* **103** (11), 1227–1246.

Veritas, D.N. 2012. *Recommended practice report DNV-RP-C207: Statistical Representation of Soil Data*, D.N. Veritas, Norway.